Published by :
http://www.ijert.org

International Journal of Engineering Research & Technology (IJERT)
ISSN: 2278-0181
Vol. 6 Issue 03, March-2017

Design of an In-pipe Inspecion Robot

Pasala Venkata Satish
Mechanical Engineering
Pydah Kaushik College of Engineering & Technology
Visakhapatnam, India

Samanthula Naveen kumar
Mechanical Engineering
Pydah Kaushik College of Engineering & Technology
Visakhapatnam, India

Sri Harsha Dorapudi
Assistant Professor,
Dept. of Mechanical Engineering
MVGR College of Engineering (A)
Visakhapatnam, India

Hepsiba Seeli
Assistant Professor,
Dept. of Mechanical Engineering
Pydah Kaushik College of Engineering & Technology
Visakhapatnam, India

***Abstract*— This paper deals with a design and motion planning of an In-pipe robot. The robots which are currently on move don't possess ability to travel in pipe while medium is on stream, thus this robot is planned with a specific end goal to conquer this issue. This is an amphibious robot hence it can travel in both liquid and gaseous environment.**

Keywords—*Inspection Robot, Kinematics, Optimal Design, Pipeline Robot, Reconfigurable robot, Motor drives, Aurdino, Amphibian robot. Service robot.*

I. INTRODUCTION

Pipelines are the medium through which large amount of fluids and gases are transferred from one place to other places every-day. Repairing those pipes has always a problematic due to geometrical and geographical difficulties. In-pipe robot inspection and repairing is a perfect solution for resolving this type of issues. In-pipe robots are classified in several ways. They are categorized as wheel track inch worm walking and pig depending on their kinematic mechanisms.

Using caterpillar wheel mechanism the robot can overcome the problem of kinematic restrictions which are occurred due to the complexity of the pipe geometries. Other robots like Flat robot [1] and snake robots [2] uses lot of servos and makes noises. The stability of these robots are quite less which makes them very less preferable, hence in this robot additional actuators like springs are used to stabilize the robots. This robot contains six motors and three of them are used to navigate robot and the other remaining motors are used to steer the robot. The robot base wheels axis is not constant they can change its axis of orientation according to the pipe geometry and environment. This can be done with a special mechanism which is later explained in this paper in design section. This unique mechanism allows robot to navigate even in the most complex geometric environment of pipeline. A versatile in-pipe robot adjust to a channel's inward surface with springs just, no extra actuators are utilized. In-pipe robots that adjust to tunnels effectively, in any case, can travel more successfully than the older robots.

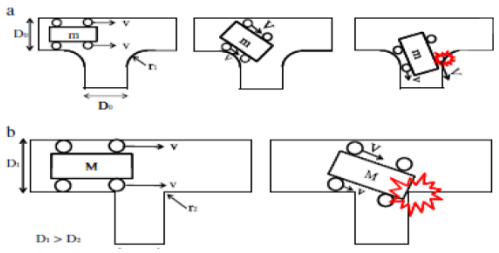

Fig 1.1: General design Problem encountered by a conventional in-pipe robot

And the channel is controlled with extra actuators. A considerable lot of the created in-pipe robots can cross straightforward channel arrangements, for example, straight pipes or pipes with no variety in distance across. Albeit, a few robots can go through fanned and elbow channels, going in spread tunnels is still viewed as a test in the field [3] of In-pipe apply autonomy. Indeed, even these robots that are intended to go through branched pipes.

II. DESIGN AND ANALYSIS

A. Design of robot central body.

Balance and friction of the robot varies with vary in the medium of the pipeline, hence an amphibious robot is best preferred for in-pipe inspection. Its design allows to blend in with surrounding environment. With simple assembly steps and dissembling steps anyone can operate it with-out a special skills. This robot central body have 3 slot inputs at left side, right side and on top side which are shown in the figures 2.1.1 and 2.1.2. In this slots the robot arms are fitted and screwed hence, with this design a single robot can handle dual environment without any help of other robots.

This key feature proves its versatility and other advantages. Those are main views of robot central body. Further design details are show in the other section of the paper

International Journal of Engineering Research & Technology (IJERT)
ISSN: 2278-0181
Vol. 6 Issue 03, March-2017

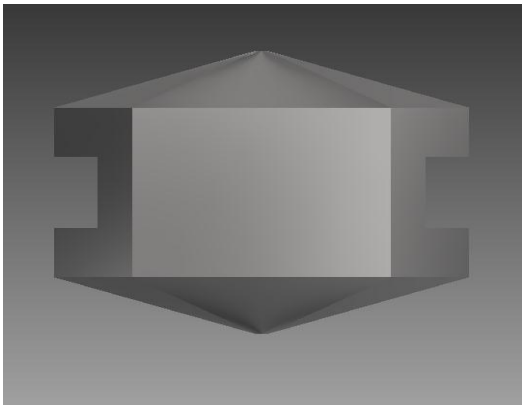

Fig 2.1.1: Bottom view of robot central body.

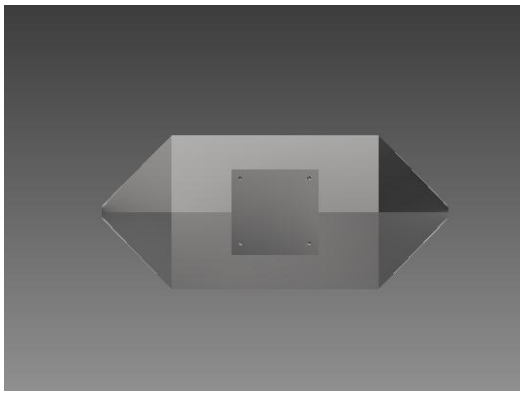

Fig 2.1.2: Right side view of robot central body.

B. Design of other essential components.

1) Robot arm

This mechanism contains three limbs, which supports the robot. These three arms connected to the main body with the help of the semi-permanent base plates. These can removed or attached by simple screws. The design is shown in figure 2.2.1. These robot arms are well tested and analyzed in order to sustain the working pressure of the stream. The stress analysis results are positive. It can sustain at the working pressure and those simulation is shown in figure 2.2.2. The extended part from the cylinder surface is used to connect the suspension and arm with Clevis pin. The whole stress will be concentrated at that area, hence in order to decrease stress concentration contact area is increased.

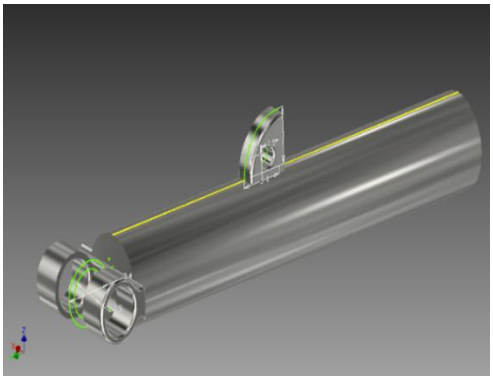

Fig: 2.2.1 Robot arm

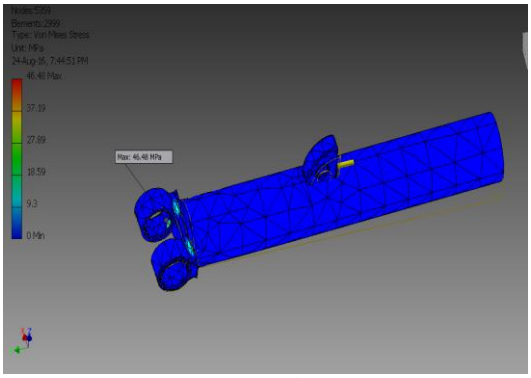

Fig: 2.2.2: Stress analysis of robot arm.

2) Suspension of robot arm for adittional actuation.

The suspension system is used to maintain necessary traction force. Thus it helps to stabilize the robot motion in pipeline. Otherwise robot losses its grip in pipe line due to stream. The stress analysis results are positive. It can sustain at the working pressure. The maximum stress concentration of 13 Mpa of pressure is observed at the junction of the arm and collar. When a maximum pressure of 500 newton's applied the deformation is very low i.e. less than 1 mm. this deformation cannot pose trouble to robot. The design and stress analysis simulation of suspension are shown in figure 2.2.3 and 2.2.4.

Fjg: 2.2.3 Suspension for robot arm.

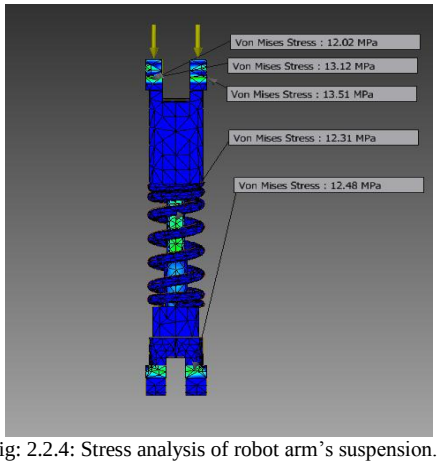

Fig: 2.2.4: Stress analysis of robot arm's suspension.

International Journal of Engineering Research & Technology (IJERT)
ISSN: 2278-0181
Vol. 6 Issue 03, March-2017

3)Caterpiller wheel base.

This robot have to go through numerous elbows or T-junctions utilizing the Caterpillar wheels. A normal wheel system can't work appropriately in the pipeline with a little range of arch in light of the fact that, occasionally, the wheels lose contact with the surface. All Caterpillar wheels keep up contact with the surface of the pipeline. The robot works steadily as each Caterpillar works autonomously.

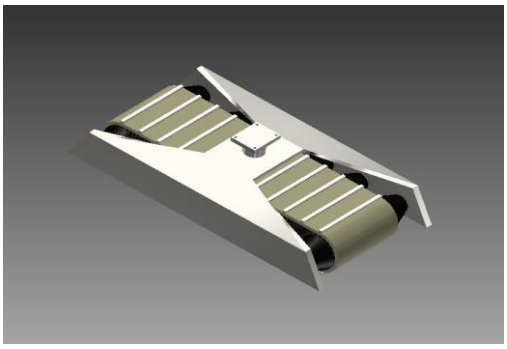

Fig 2.2.6: Caterpillar wheel base

C. Design of fully assembled Robot.

In this configuration three arms are attached to the central body by means of screw at three different sides. Each arm have a caterpillar wheels and in order to maintain stability in movements suspensions are also additionally added to the robot arm. The full assembled robot is shown in the figure 2.3.1. And its kinematic equations and motion planning are elaborated in section 3 and section 4.

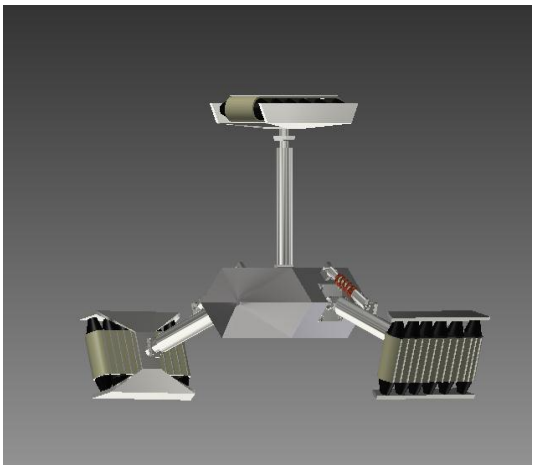

Fig 2.3.1: Robot after assembly

III. KINEMATIC EQUATIONS OF ROBOT

A. Kinematic equations of robot in mode gaseous configuration mode.

1) Overcoming gravity

The base typical power required for the robot to defeat gravity is

$$\mathbf{N\ min = mg/2\mu}$$

The robot have to travel in both vertical and horizontal axis of the pipeline hence, the force required for it to move will changes with change in axis and in order to travel in a stable state, it should first overcome its own body weight i.e it should overcome gravity. μ and g are the coefficient of grinding and the speeding up of gravity, individually. To affirm with the parameters set to those could apply a power higger than the base power required, determined a condition for the ordinary power applied by the two springs (N spring).

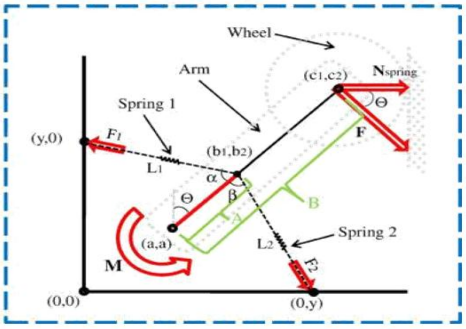

Fig 3.1.1: Free body diagram of robot arm.

$$X_{d1} = L_1 - X_1 \quad (1)$$

$$X_{d2} = L_2 - X_2 \quad (2)$$

$$b_1 = a + A \text{ transgression } \Theta \quad (3)$$

$$b_2 = a + A \cos \Theta \quad (4)$$

$$L_1 = \sqrt{b1+(y-b_2)^2} \quad (5)$$

$$L_2 = \sqrt{(y-b_2)2+b2^2} \quad (6)$$

$$\alpha = \cos^{-1}((A^2 + L_1^2) - (y-a)^2 - a^2/2L_1A) \quad (7)$$

$$\beta = \cos^{-1}((A^2 + L_2^2) - (y-a)^2 - a^2/2L_2A) \quad (8)$$

x_{d1}, x_{d2}, and x_i signify the prolonged lengths of spring 1 and spring 2 and the underlying length of the spring. On the off chance that x_{d1} or x_{d2} gets to be shorter than zero, the quality ought to be set to zero, in fact that the springs apply no power on the arm in these cases. The conditions for the minute on the pivot (an, an) applied by two springs and the typical power created by the springs.

$$M = kA(X_{d2}\sin\beta - X_{d1}\sin\alpha) \quad (9)$$

$$N \text{ spring} = F\cos\theta = M/B\cos\theta \quad (10)$$

The above equation gives the relationship between the N normal force and mass M and the angle θ, hence in order to overcome gravity the necessary variable are substituted and the required N will be sorted out.

2) Kinemtaic equations of motion for robot.

$$v_2 = r\dot{\theta}_2. \quad (11)$$

$$v_3 = r\dot{\theta}_3. \quad (12)$$

To begin with, we expect that each caterpillar wheel holds a line contact at the internal mass of the pipeline, and that the wheel does not slip in the even course and does not turn about the z-hub, but rather is permitted to move along the z-pivot. The power created by the mounted micro-motor is transmitted to the caterpillar wheel through a slant gear. We characterize θ_1, θ_2, and θ_3 as the pivoting points of the caterpillar wheels; r indicates the sweep of the wheel, and a means the range of the robot body. At that point, the straight speeds v_1, v_2, and v_3 at the focal point of the wheels are given by

$$v_1 = r\dot{\theta}_1$$

International Journal of Engineering Research & Technology (IJERT)
ISSN: 2278-0181
Vol. 6 Issue 03, March-2017

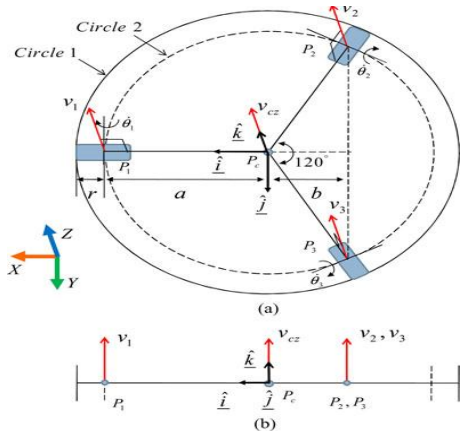

Fig 3.1: (a) Cross-sectional view of the pipeline. (b) Velocity profile at the side view of the pipeline.

The straight speeds v_1, v_2, and v_3 have diverse magnitude of velocities at elbows or T-branches. At that point, the straight speed at the middle Pc of the robot is signified as v_{cz} , and the rotational speeds about the body is ˆi and ˆj are meant as ω_x and ω_y . At that point, so as to infer the kinematic relationship between the information speed ($\dot{\theta}_1$, $\dot{\theta}_2$, and $\dot{\theta}_3$) and the yield speed (ω_x, ω_y , and v_{cz}), we break down the parts of the yield speed for four cases. Fig. 3.1 (a) and (b) demonstrates the cross-sectional perspective of the pipeline and the speed profile along the edge perspective of the pipeline, individually.

Case 1 ($v_1 = v_2 = v_3$): Case 1 is the state in which the robot moves in the straight pipeline. As appeared in Fig.3.1: (a), the three wheels speeds are equivalent; consequently, the direct speed v_{cz} at the middle can be depicted as

$$v_{cz} = v_1 (= v_2 = v_3) \quad (13)$$

The rotational velocities ω_x and ω_y didn't exist.

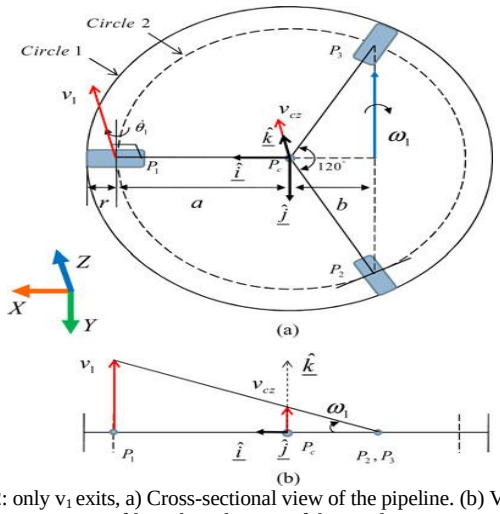

Fig 3.2: only v_1 exits, a) Cross-sectional view of the pipeline. (b) Velocity profile at the side view of the pipeline

Case 2 (Only One Velocity Exists (v1): case 2 is the state where one and only speed exists, For this situation, the focuses P_2 and P_3 are stationary, and at the point P1, a direct speed v_1 is produced. At that point, the straight speed at the middle Pc of the robot is acquired by geometric investigation. Resultantly, the robot pivots about the line P_2, P_3 with the rotational speed ω_1 given by the following equations

$$\omega_1 = v_1 /(a + b) \quad (14)$$

Since $b = a \cos 60^\circ$, (3) becomes

$$\omega_1 = v_1/(1.5)a \quad (15)$$

The straight speed v1 is created by turn of the caterpillar wheel, which can be written as

$$v_1 = r\dot{\theta}_1 \quad (16)$$

The rotational velocity vector ω_1 with respect to the local co-ordinate of the robot can been written as

$$\omega_1 = -\, r/(1.5a)\, \dot{\theta}_1 \quad (17)$$

The rectilinear components of $\omega 1$ can be written as

$$\omega_x = 0 \quad (18)$$

$$\omega_y = -\, r/(1.5a)\theta_1 \quad (19)$$

Linear velocity v_{cz} at the center of the robot is

$$vcz = b/(a + b) = v_1 = 0.5a/(1.5a)v_1 = r3\dot{\theta}_1 \quad (20)$$

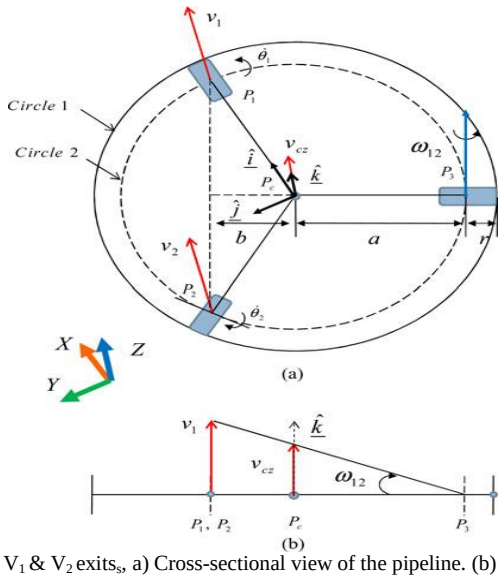

Fig 3.3: V_1 & V_2 exits, a) Cross-sectional view of the pipeline. (b) Velocity profile at the side view of the pipeline

Case 3 (Two Velocities Exist (v_1, v_2)): Case 3 is the state in which two speeds exist, For this situation, the point P_3 is stationary, and at the points P_1 and P_2 , the straight speeds v_1 and v_2 are created. At that point, the direct speed at the middle Pc of the robot is gotten by geometric investigation. Resultantly, the turn speed ω_{12} is created by the straight speed v_1 and v_2 .when the direct speeds v_1 and v_2 are the same, the rotational speed ω_{12} is given by

$$\omega_{12} = v_1/(a + b) = v_1/(1.5a) \quad (21)$$

The rotational velocity vector $\omega 12$

$$\omega_{12} = r\theta_2/(\, 1.5a(\cos 30^\circ \hat{i} - \sin 30^\circ \hat{j}))$$

$$\omega_{12} = \sqrt{(3r/3a)}\theta_2 \hat{i} - r3a\dot{\theta}2\hat{j} \quad (22)$$

$$v_{cz} = a/(a + b)v_1 = a/(1.5a)v_1 = 2r/3(\theta_1) \text{ or } 2r/3(\theta_2) \quad (23)$$

Case 4 (v1 = v2 = v3): Case 4 is the state where three speeds exist together with various qualities (e.g., $v_3 < v_2 < v_1$). For this situation, the rotational speed vector of the robot is equivalent

International Journal of Engineering Research & Technology (IJERT)
ISSN: 2278-0181
Vol. 6 Issue 03, March-2017

to the summation of the rotational speed vector made by the straight speed of every wheel. That is to say, when just v_1 exists, the rotational speed vector is indistinguishable to (19). Additionally, when just v_2 exists, the rotational speed vector is as per the following:

$$\omega_2 = r\dot{\theta}_2/1.5a\ (\cos 30^\circ \hat{i} + \sin 30^\circ \hat{j}) = \sqrt{3}r/3a(\dot{\theta}_2 \hat{i}) + r/3a(\dot{\theta}_2 \hat{j},) \quad (24)$$

Where $\omega_x = (\sqrt{3}r/3a)\dot{\theta}_2$, and $\omega_y = (r/3a)\dot{\theta}_2$.

$$\omega_2 = r\dot{\theta}_3/1.5a\ (-\cos 30^\circ \hat{i} + \sin 30^\circ \hat{j}) = -\sqrt{3}r/3a\dot{\theta}_3 \hat{i} + r/3a\dot{\theta}_3 \hat{j}, \quad (25)$$

Where $\omega_x = -(\sqrt{3}r/3a)\dot{\theta}_3$, and $\omega_y = (r/3a)\dot{\theta}_3$.
Assuming that v_1, v_2, and v_3 exist at the same time,

$$\omega = \omega x \hat{i} + \omega y \hat{j} \quad (26)$$

$$\omega x = \sqrt{3}r/3a(\dot{\theta}_2) - \sqrt{3}r/3a(\dot{\theta}_3) \quad (27)$$

$$\omega y = -(2r/3a)\dot{\theta}_1 + (r/3a)\dot{\theta}_2 + (r/3a)\dot{\theta}_3 \quad . (28)$$

The velocity v_{cz} at the center of the robot is given as

$$v_{cz} = 1/3(v_1 + v_2 + v_3) = r/3(\dot{\theta}_1 + \dot{\theta}_2 + \dot{\theta}_3) \quad (29)$$

Finally, the relationship between the input velocity vectors which are obtained is as follows
$\dot{\theta}_a = (\dot{\theta}_1\ \dot{\theta}_2\ \dot{\theta}_3)^T$ and the output velocity vector
$\dot{u} = (\omega_x\ \omega_y\ v_{cz})^T$ is constructed as

$$\dot{u} = [G_{ua}]\ \dot{\theta}_a \quad (30)$$

Combining (15) and (18). Here, the Jacobian is given as

$$[G_{ua}] = \begin{matrix} 0 & \sqrt{3}r/3a & -\sqrt{3}r/3a \\ -2r/3a & r/3a & r/3a \\ r/3 & r/3 & r/3 \end{matrix} \quad (31)$$

For a given direct speed (vcz) and rotational speeds (ωx and ωy) at the focal point of the robot, the precise speed of the wheels are computed as

$$\dot{\theta}_a = [G_{ua}]^{-1}\ \dot{u}. \quad (32)$$

The pivot angle of every wheel is obtained by numerical integration of (32).

IV. MOTION PLANNING.

Few analyses were done to check movement ability of the robot at 45 and 90 degrees elbows and Tee -branches. At 45 and 90 degrees elbow, there are 3 sorts, at T-branch, there are 16 sorts, of movements. Distinctive sorts of robot movement in various pipeline twists 45 and 90 degrees elbows, and T-branches) are shown in fig 4.1 below.

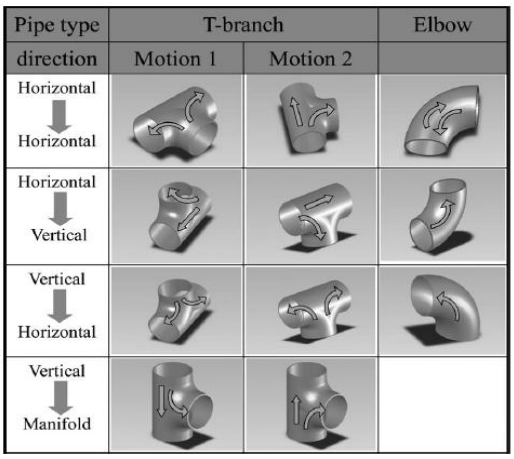

Fig 4.1: Different motions in elbow & T -branches.

A. *Motion planning at 90 degrees elbow and T-branch.*

The movement arranging of the robot at 90 degree elbow is given in Fig. 4.2. The robot make a turn by making stationary the wheels reaching the internal corner of the 90 degrees elbow and pivoting the wheels reaching the external side of the 90 degrees elbow toward vertical or even heading it expects to turn. The motion of the robot at T-branch is given in Fig.4.3 it has been seen that movement arranging at T-branch is more difficult because there are numerous ways at the T-junction. The turning from flat to the vertical axis inside the pipeline is difficult. This is because of the low contact for the caterpillar wheels to have the capacity to reach to within limits of the pipeline

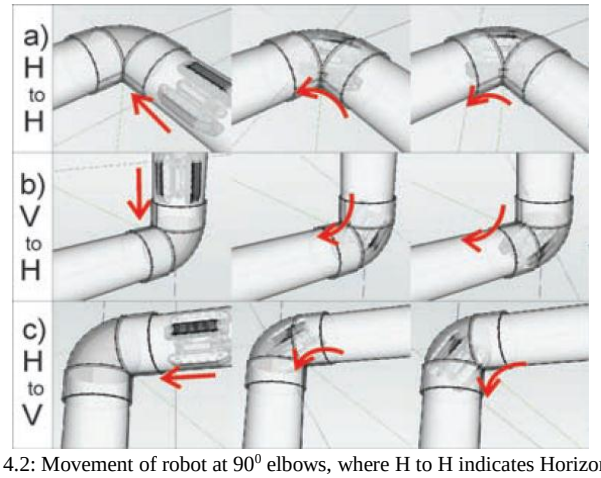

Fig 4.2: Movement of robot at 90^0 elbows, where H to H indicates Horizontal to Horizontal, V to H indicates Vertical to Horizontal, and H to V indicates Horizontal to Vertical motion.

At this point when there is a less area of contact, the robot wheels can't have any significant bearing the usefulness of separating the caterpillar's pace for making a turn.
In the situations which described in figures, the robot can make a turn by making the wheels stationary reaching the internal corner of the T-branch and pivoting the wheels reaching the external corner of the T-branch toward the vertical side.

International Journal of Engineering Research & Technology (IJERT)
ISSN: 2278-0181
Vol. 6 Issue 03, March-2017

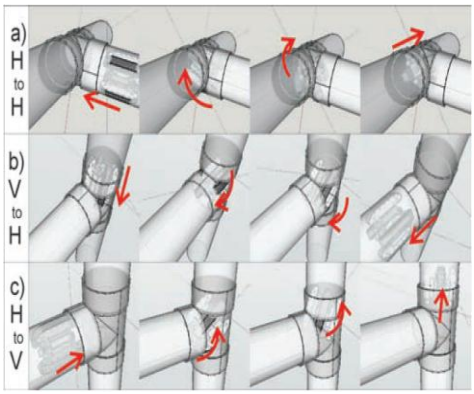

Fig 4.3: Motion planning at T-branch

V. EXPERIMENT.

The Prototype of scale 1:4 is prepared for testing the design and working capabilities. For the trial assessment, the robot is utilized in the examination of a complex pipeline design that has been developed utilizing all accessible pipeline fittings that a regular pipeline framework utilizes, where the robot additionally needs to perform vertical and horizontal movement. Review that one of such complex pipeline format utilized as a part of the investigations is given in Fig. 4.1. The robot is initially tested in every curves separately and afterward tested to the entire pipeline format. The robot figures shows that how to go through these pipes by changing the servo motor speed suitably.

A. Motion at 90 elbow.

The Fig. 5.1 demonstrates that the pipeline inspection robot is heading out to numerous movements in several axis (moving up and down in the vertical pipeline) in the 90 degrees elbow of the trial pipeline format (movement at 45 degrees elbow is similar to 90 degrees).

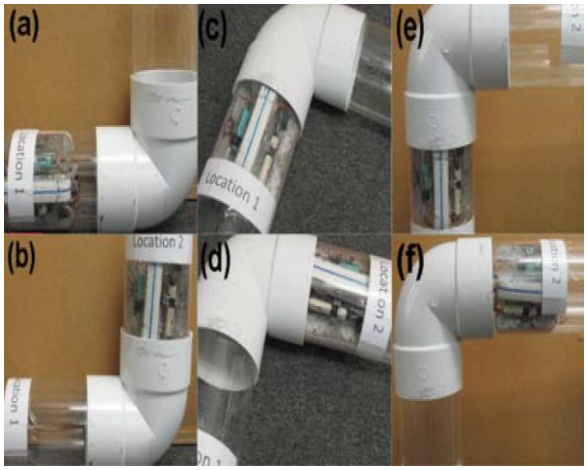

Fig 5.1: Types of motion at 90 degrees elbow, where (a), (b) show H to V, (c), (d) show H to H, and (e), (f) show V to H motion.

B. Motion at T-junction..

The Fig. 5.2 demonstrates that the robot setting out to a few turnings in a T-branch of the exploratory pipeline design. The movement of individual caterpillar wheels with different speed rate with programmed motion planning helps in maneuvering these complex pipeline geometry. Thus it proves that the design is compact and efficient.

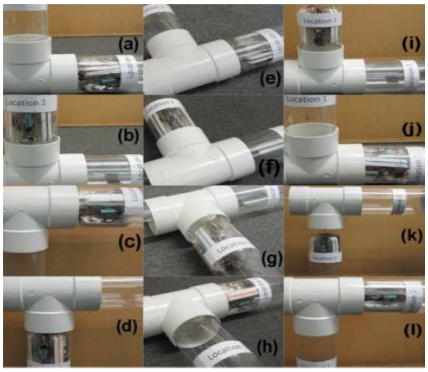

Fig 5.2: Types of motion at T-branch, where (a)-(d) show H to V, (e)-(h) show H to H, and (i)-(l) show V to H motion.

VI. CONCLUSION

With the help of various experimental results, the design and movement planning of this robot is perfected. Thus it can be utilized for pipeline inspection, exploration in sewage tunnels and other industrial pipe lines [4].

The designed pipeline inspection robot which is shown in figure 2.3.1 can inspect 15–25 Inch pipelines while this prototype is used to inspect the medium pipelines of sizes below 200 mm diameter. Robot module comprises of three sets of caterpillar wheel base, each of which is worked by a small dc motor. Free control of each Caterpillar wheels permits, directing ability through elbows or T-branches cross-sectional area. And by adding some additional sensors [5] this robot can detect leakages and can save people and economy from blasts.

VII. ACKNOWLEDGMENT .

I wish to thank Hepsiba seeli, Sri Harsha Dorapudi, S Naveen kumar and other college Faculty member's along with our lab technicians.

VIII. REFERENCES.

[1] T. Oya and T. Okada, "Development of a steerable, wheel-type, in-piperobot and its path planning," *Adv. Robot.*, vol. 19, no. 6, pp. 635–650,2005.

[2] A. A. Transeth and K. Y. Pettersen, "Snake robot obstacle-aided locomotion: modeling, simulations, and experiments," *IEEE Trans. Robot.*,vol. 24, no. 1, pp. 88–104, Feb. 2008.

[3] H. Roth, K. Schiling, S. Futterknecht, U. Weigele, M. Risch, "Inspection and repair robots for waste water pipes, a challenge to sensories and locomotion", Proc. of IEEE International Conference on Robotics and Automation, pp. 476-478, 1998.

[4] T. Okada, T. Sanemori, MOGRER: a vehicle study and realization for in-pipe inspection tasks, IEEE Journal ofRobotics and Automation 3 (1987) 573–582.

[5] "Remote detection and localization of gas leaks with autonomous mobile inspection robots in technical facilities" website: http://www.flir.com/cs/emea/en/view/?id=62559.